ARMY RESEARCH LABORATORY

Tunable TiO_2 Nanotube Arrays for Flexible Bio-Sensitized Solar Cells

by Joshua J. Martin, Mark H. Griep, Anit Giri, Samuel G. Hirsch, Victor Rodriguez-Santiago, Andres A. Bujanda, James E. McCauley, and Shashi P. Karna

ARL-TR-6075 **August 2012**

NOTICES

Disclaimers

The findings in this report are not to be construed as an official Department of the Army position unless so designated by other authorized documents.

Citation of manufacturer's or trade names does not constitute an official endorsement or approval of the use thereof.

Destroy this report when it is no longer needed. Do not return it to the originator.

Army Research Laboratory
Aberdeen Proving Ground MD 21005-5069

ARL-TR-6075 **August 2012**

Tunable TiO_2 Nanotube Arrays for Flexible Bio-Sensitized Solar Cells

Joshua J. Martin, Mark H. Griep, Anit Giri, Samuel G. Hirsch, Victor Rodriguez-Santiago, Andres A. Bujanda, James E. McCauley, and Shashi P. Karna
Weapons and Materials Research Directorate, ARL

REPORT DOCUMENTATION PAGE	Form Approved OMB No. 0704-0188

1. REPORT DATE *(DD-MM-YYYY)*	2. REPORT TYPE	3. DATES COVERED (From - To)
August 2012	Final	3 June 2011–26 August 2011

4. TITLE AND SUBTITLE
Tunable Tio_2 Nanotube Arrays for Flexible Bio-Sensitized Solar Cells

5a. CONTRACT NUMBER

5b. GRANT NUMBER

5c. PROGRAM ELEMENT NUMBER

6. AUTHOR(S)
Joshua J. Martin, Mark H. Griep, Anit Giri, Samuel G. Hirsch, Victor Rodriguez-Santiago, Andres A. Bujanda, James E. McCauley, and Shashi P. Karna

5d. PROJECT NUMBER
622618

5e. TASK NUMBER

5f. WORK UNIT NUMBER

7. PERFORMING ORGANIZATION NAME(S) AND ADDRESS(ES)
U.S. Army Research Laboratory
ATTN: RDRL-WMB-D
Aberdeen Proving Ground MD 21005-5069

8. PERFORMING ORGANIZATION REPORT NUMBER
ARL-TR-6075

9. SPONSORING/MONITORING AGENCY NAME(S) AND ADDRESS(ES)

10. SPONSOR/MONITOR'S ACRONYM(S)

11. SPONSOR/MONITOR'S REPORT NUMBER(S)

12. DISTRIBUTION/AVAILABILITY STATEMENT
Approved for public release; distribution is unlimited.

13. SUPPLEMENTARY NOTES

14. ABSTRACT
Highly ordered, free-standing titanium dioxide nanotube (TiNT) arrays have been of intense interest to the alternative energies field in recent years due to their barrier-free electron conduction pathway vs. TiO_2 nanoparticles in dye-sensitized solar cell (DSSC) designs. TiNT arrays prepared by electrochemical anodization of Ti foils and combined with a transparent, Indium Tin Dioxide coated PET film are attractive candidates for efficient, flexible DSSC's. Flexible solar cells offer great benefits because of the potential for low-cost, roll-to-roll production and the increase in applications due to superior robustness. This approach utilizes a two-step anodization procedure coupled with implementation of a rapid inert gas dehydration and ultrasonic agitation detachment method. By controlling the reaction conditions during anodization (voltage, duration, concentration), TiNT arrays with specific morphology, lengths, and diameters can be tailored to satisfy a particular application such as incorporating specialized protein dyes—in particular, bacteriorhodopsin. The free-standing arrays comprised of hexagonally closed-packed and regularly ordered TiNT membranes have been synthesized and detached from the original Ti substrate. Once the TiO_2 sol-gel is created, the free-standing arrays will be attached to the flexible PET film for improved photovoltaic properties and overall performance.

15. SUBJECT TERMS
bacteriorhodopsin, dye-sensitized solar cell, BSSC, tunable TiO_2, titanium dioxide nanotubes

16. SECURITY CLASSIFICATION OF:			17. LIMITATION OF ABSTRACT	18. NUMBER OF PAGES	19a. NAME OF RESPONSIBLE PERSON
a. REPORT	b. ABSTRACT	c. THIS PAGE			Mark Griep
Unclassified	Unclassified	Unclassified	UU	24	19b. TELEPHONE NUMBER (*Include area code*) (410) 306-4953

Contents

List of Figures

Acknowledgments

We thank Dr. Raymond Mackay and Dr. Daphne Pappas for their aid and technical input.

INTENTIONALLY LEFT BLANK.

1. Introduction and Background

Soldiers and vehicles are constrained by a dependence on bulky batteries to meet their power needs. Future Force Soldiers will be equipped with a wide-array of technology, essentially all requiring electrical power for operation. Integrating solar harvesting capabilities with future equipment would relieve the burden of batteries and increase overall performance of Soldiers. While modern silicon cells are costly to produce and adversely affect mobility, dye-sensitized solar cells (DSSCs) offer very advantageous properties. These systems are potentially capable of achieving higher efficiencies at much reduced costs, have a lower environmental impact, and are easier to fabricate and manufacture than current silicon solutions. Dye-sensitized titanium dioxide (TiO_2) platforms do not require expensive semi-conductor substrates or highly complex processing steps—making roll to roll production possible (*1*). Most importantly, they can be geared to be highly robust and flexible. These attributes qualify DSSC's as an attractive candidate for future solar energy harvesting systems.

The objective of this research is to develop TiO_2 nanotubes and investigate their application in a flexible DSSC. A particular focus of this work is to grow highly ordered nanotube arrays with tunable pore diameters in order to compensate for a bacteriorhodopsin (bR) protein dye.

1.1 DSSC Overview

The classic DSSC is generally composed of a layer of nanocrystalline TiO_2 particles on a conducting substrate, a platinum counter electrode, an electrolyte, and an adsorbed Ru dye as a sensitizer (*2*). The cell presented in this research is unique as it utilizes TiO_2 nanotubes sensitized with a photoactive protein—bacteriorhodopsin dye. In contrast to conventional silicon systems, where the semiconductor assumes both the light absorption and charge carrier transport, the two functions are separated (*3*). The operating principle is demonstrated in figure 1. On the surface of the TiO_2 is an adsorbed dye, attached by specific functional groups, which serves as a light absorber and photon to electron converter.

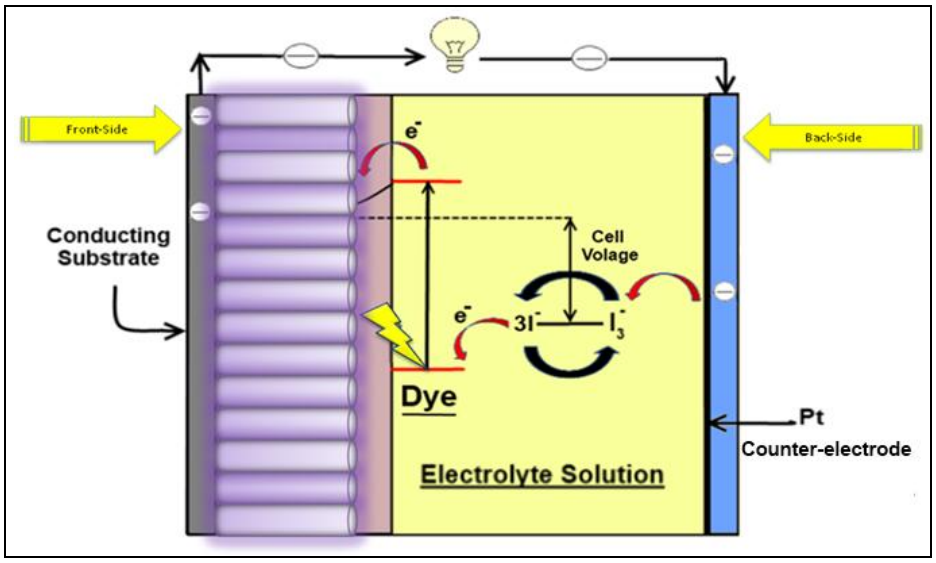

Figure 1. Principle of a DSSC.

A key requirement for the dye is that the lowest unoccupied molecular orbital (LUMO) of the dye molecule is energetically positioned slightly higher than the conduction band of TiO_2. Under the illumination of sunlight, the highest occupied molecular orbital (HOMO)-LUMO transitions in the dye occur. Photo-excitation of the dye leads to rapid injection of electrons into the TiO_2. These electrons are then transferred to the conducting electrode. For typically used Ru dyes, the electron injection from the dye sensitizer to the conduction band of TiO_2 occurs through a metal-to-ligand charge transfer (MLCT) pathway (*4*). Electron donation from the redox couple in the electrolyte, usually an ionic liquid containing an I_3^-/I system, regenerates the oxidized dye and returns it to its original state. The tri-iodide ions formed in the dye regeneration process diffuse through the liquid phase to the cathode, where they are reduced back to iodide ions to complete the cycle (*5*). The efficiency of collection of the photo-injected electrons, which is a critical factor in device performance, is determined by competition between electron transport to the anode and electron transfer to the I_3^- ions in electrolyte. To date, results of light-to-electricity conversion efficiencies of 11% have been reported in literature (*6*).

While this demonstrates much prospect, the electron transport time in TiO_2 nanoparticles is relatively slow when compared to the rate of de-excitation of the dye and the regeneration time constant of the dye (*7*). Electron flow is slowed down due to defects, surface states, grain boundaries, and other electron trapping sites within the nanoparticles. These factors enhance recombination and adversely affect electron transfer (*8*). In order to minimize this effect, the use of more organized TiO_2 structures such as nanotubes has been proposed in recent years (*9*).

TiO_2 nanotubes have a highly-ordered structure with vertical pore geometry, which appears to be optimal for the fabrication of solid-state junction cells (*10*). This is due mainly to the one dimensional (1-D) conductive path of nanotubes vs. the three-dimensional (3-D) unsystematic

walk network and grain boundary effects associated with randomly organized nanoparticles, displayed in figure 2. It has been recently shown that compared to conventional TiO_2 nanoparticle films of the same thickness, TiO_2 nanotube arrays give enhanced light scattering and improved collection efficiencies (*9*). Figure 3 shows the BSSC design.

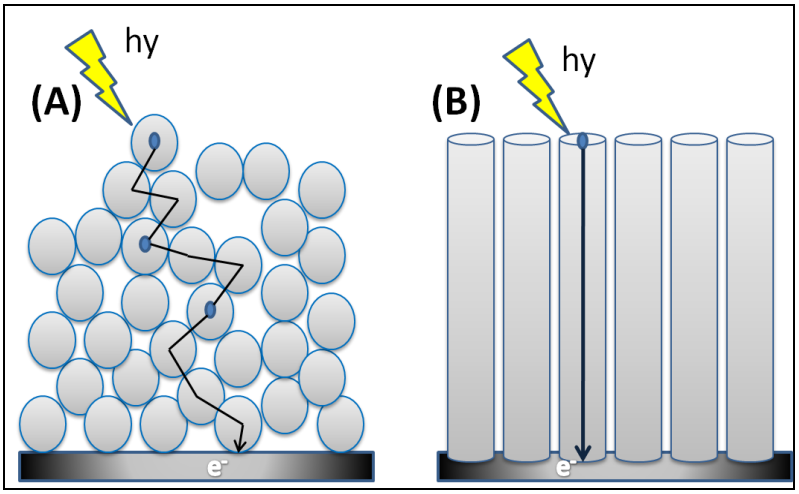

Figure 2. (A) Random electron path through nanoparticles and (B) direct electron transport in nanotubes.

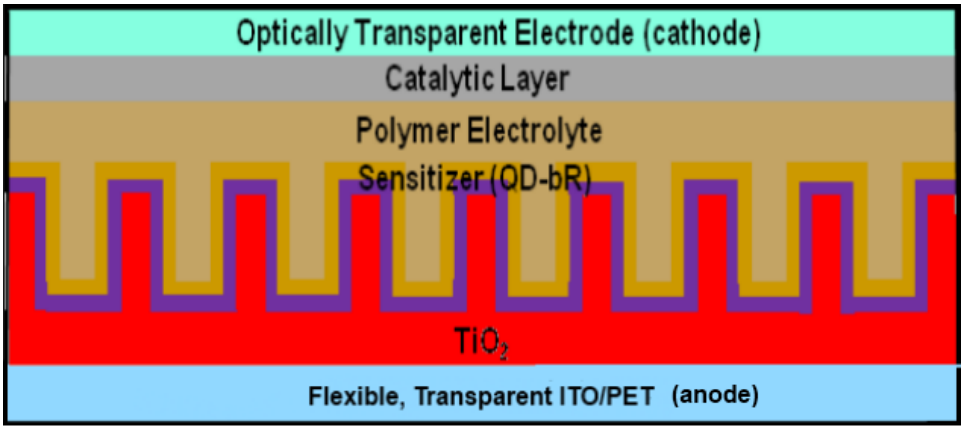

Figure 3. BSSC design.

1.2 Critical Factors for Efficiency

The conversion efficiency of DSSC's is mainly governed by: (1) molar absorption coefficient and HOMO-LUMO levels of the dye, (2) the effective surface area of the electrodes available for dye anchoring, (3) the transport kinetics of electrons to the substrate, (4) the efficiency of dye regeneration via a redox couple, and (5) the losses arising from recombination and back reactions of injected charge carriers (*11*). Critical optimization factors pertaining to the TiO_2 arrays will be outlined, with a particular focus in maximizing pore diameter to accommodate for the bR dye.

The performance of TiO_2 nanotube arrays in a DSSC as an efficient semi-conductor and electron recipient is directly related to several factors: morphology, crystallinity, and geometry (*2*). A number of studies have been conducted in order to control the dimensions of TiNT arrays via anodic oxidation (anodization). Uniform TiO_2 nanotube arrays with various lengths, diameters, and wall thicknesses can be fabricated in fluoride containing solutions (HF and NH_4F) by tailoring the electrochemical conditions (anodization voltage, fluoride concentration, anodization time, and temperature) (*12–14*).

1.2.1 Growth of TiO_2 Nanotube Arrays

The simple electrochemical process of anodizing Ti foils (displayed in figure 4) to produce TiNT's can be accomplished using a two (or three) electrode system utilizing Ti-foil as the working electrode (+), a counter electrode such as platinum (-), and a voltage source. Nanotube formation in fluoride-ion-bearing electrolytes occurs due to three simultaneously occurring processes: electric field assisted oxidation of Ti metal to form TiO_2, the field assisted dissolution of Ti metal ions in the electrolyte, and the chemical dissolution of Ti and TiO_2 due to etching by fluoride ions (which is substantially enhanced by fluoride ions) (*15*). A thin dioxide film develops at the Ti/electrolyte interface due to the following chemical reaction (*9*):

$$Ti + 2H_2O \rightarrow TiO_2 + 4H^+ - 4e^- \quad (1)$$

As this mechanism occurs, one can note that the current measured will reduce as time goes on. This is due to the increase in resistance provided by the oxide. As the oxygen ions (O^{2-}) are transported from the solution to the Ti, titanium ions (Ti^{4+}) transported from the titanium to the electrolyte interface are dissolved into the solution. A simultaneous reaction occurs at the TiO_2/electrolyte interface forming soluble fluoride complexes. These create pits at the surface according to the following reaction (*9*):

$$TiO_2 + 6F^- \rightarrow TiF_6^{2-} \quad (2)$$

These complexes dissolve and form pits on the surface of the newly formed TiO^2. As anodization time increases, all three processes continuously increase the depth of the pores (pits) and therefore produce highly ordered nanotubes (*16*).

1.2.2 Length, Diameter, and Pore Size

Certain geometrical parameters of the nanotube arrays have a large effect on performance. These parameters can be tuned by controlling the anodization conditions. Length, diameter, and pore size (inner diameter) are largely influenced by anodization time, voltage, and NH_4F concentration (*17*). Increasing the overall length of the array allows for more surface area, resulting in more attached dye. The easiest way to modify the length of the array is to increase the anodization time. Due to the higher number of dye molecules that can attach to the increased length of the tubes, increasing length leads to an increase in the short circuit photocurrent. It is important to note that although the short circuit current is increased with tube length, so is the

chance of recombination and electron trapping. It has been reported that when the TiNT length is significantly more than 20 μm, the diffusion length of electrons becomes shorter than the length of the tube (*18*). Hence, the photovoltaic performance shows an initial increase and followed decrease with increasing TiO_2 nanotube length. The same study was able to achieve a conversion efficiency (Ƞ) of 8.07% using a 20.8-μm nanotube array with an open-circuit voltage (V_{OC}) of 0.814 V, a short-circuit current (J_{SC}) of 15.46 mA cm^{-2}, and a fill factor (FF) of 64.1%. This agrees with other studies that report the maximum internal conversion efficiency is achieved for tubes of a length of ~20 μm (*2*).

In order to further modify the dye "absorbing" capabilities of the nanotubes, diameter and pore size are very important. These factors are critical depending on certain situations. In order to take full advantage of nanotubes having both inner and outer walls, the dye being used must also fit inside of the inner diameter. The diameter of the tubes can be adjusted by the anodization voltage (*10*). In addition, modifying the concentration of the electrolyte used during anodization further modifies the pore diameter and wall thickness. This occurs due to the increase in the dissolution rate, which increases due to a higher amount of F^-ions within the electrolyte solution, leading to an increase of the inner diameter and thus reducing wall thickness and increasing the pore size (*9*).

1.2.3 Crystalline Structure

The crystal structure of TiO_2 tube walls is a significant factor affecting its electronic properties. When anodically formed, the TiO_2 arrays are initially in an amorphous state. Due to a large amount of defects, impurities and other recombination sites, the amorphous TiO_2 has hardly any conversion efficiency (*11*). In order to harness the maximum potential of the TiNT array, the nanotubes must be annealed to a crystallite form.

When annealed at temperatures between 300 and 500 °C for about 3 h, the anatase crystalline form of TiO_2 can be obtained. At higher temperatures, 550 °C and above, rutile-based TiO_2 will begin to develop. In addition to annealing temperature, the ramping speed has an effect on solar cell performance (*2*). High ramping speeds (greater than 30 °C /min) can adversely affect performance due to an increase in structure defects.

Little attention has been paid to the rutile form of TiO_2, although it is used as a base in most paints due to its light scattering ability. In general, a pure anatase TiO_2 nanostructure is preferred over rutile due to their superior performance in DSSC. This results from its surface chemistry and potentially higher conduction-band energy (*19*). Rutile films consist of homogenously distributed rod-shaped particles. These particles show no preferred orientation and therefore have a much smaller packing density compared to anatase-based particles. The smaller packing density results in smaller particle connectivity. In other words, electrons move slower through rutile-based TiO_2 than in anatase based. In addition, anatase arrays have a larger surface area per

unit volume (about 25%); this allows for more dye to be absorbed. As a result, anatase structures can achieve a 30% higher J_{SC} than rutile. Maintaining a pure anatase TiO_2 nanostructure is essential for achieving a high efficiency DSSC using nanotubes.

2. Materials and Experimental Procedure

TiO_2 nanotube arrays were grown using a single-step anodization process. Titanium foils (Sigma-Aldrich, 99.7%, 0.25µm) were electrochemically anodized in a standard two-electrode cell using a counter-electrode and an Agilent E3649A DC power supply (figure 4). The electrodes were kept at a fixed distance of 1.5 cm. The foils were first mechanically polished using a 9-µm diamond compound with a silk cloth and microid extender followed by a colloidal silica/wetted imperial cloth. The foil was then cut into 1- × 2-cm samples. Then, the substrates were separately sonicated in acetone, isopropanol and ethanol, each for 5 min before, being rinsed with deionized (DI) water. The anodization process was performed at 60 V for 2–6 h using an electrolyte consisting of 0.25 weight-percent NH_4F and 0.75% H_2O in ethylene glycol. The anodized samples were rinsed with DI water and then soaked in methanol for 30 s to initiate the detachment procedure. Free-standing TiNT membranes were separated from the Ti substrate by drying the methanol-wetted samples with a stream of N_2 gas. This caused the freshly-formed TiNT array to rapidly dry and delaminate from the substrate. To effectively remove the TiNT membranes, methanol wetting and N_2 blowing were repeated several times.

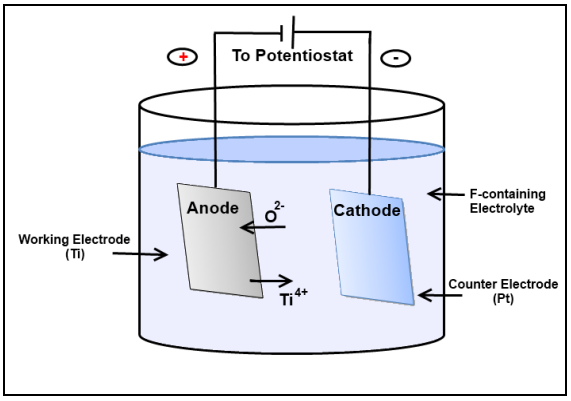

Figure 4. Anodization setup.

To crystallize the amorphous TiNT arrays into the anatase phase, a single-step annealing process was used. The TiNT arrays were heated in a tube furnace at 450 °C for 3 h using a heating rate of 20 °C s^{-1}. After annealing, the arrays are to be bonded to a PET film using a TiO_2 sol containing titanium butoxide and polyethylene glycol and sintered at a low temperature of 200 °C to keep the PET from thermally degrading.

Following the annealing process, the TiNT/PET films are to be sensitized using a bacteriorhodopsin dye (bR) for 16 h. Due to time constraints amongst other obstacles, the performance of a DSSC sensitized with bR is evaluated on a titanium substrate rather than a flexible ITO/PET film.

3. Results and Discussion

Figure 5 shows the effects of methanol wetting and N_2 blowing on freshly anodized TiNT arrays. Due to the low surface tension of methanol, soaking the TiNT arrays allows the methanol to penetrate the oxidized layer and aid in the delamination of the nanotube layer. This resulted in a nanotube array nearly twice the size of one collected without methanol wetting.

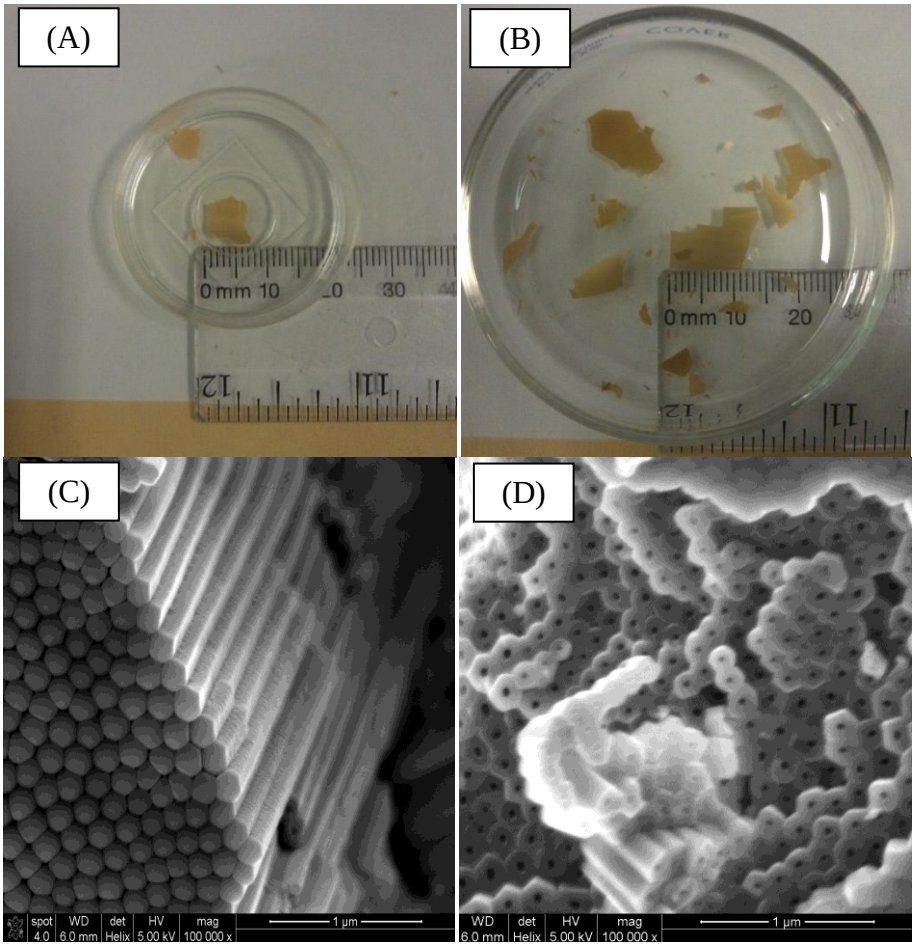

Figure 5. (A) Effects without methanol wetting, (B) effects with methanol wetting, (C) side SEM view of hexagonal, highly-oriented nanotube array, and (D) top view.

SEM images in figure 5 (C and D) show highly aligned, densely packed, hexagonally oriented nanotube arrays. This result was surprisingly unexpected because the arrays were formed using a single step anodization procedure. Figure 6 reveals that the hexagonally aligned nanotubes also exhibit bamboo-like rings. Although this has been seen before, the standards in literature believe these rings are formed by alternating (or stepping) the applied voltage. However, these highly organized arrays were anodized at a constant 60 V for 3 h.

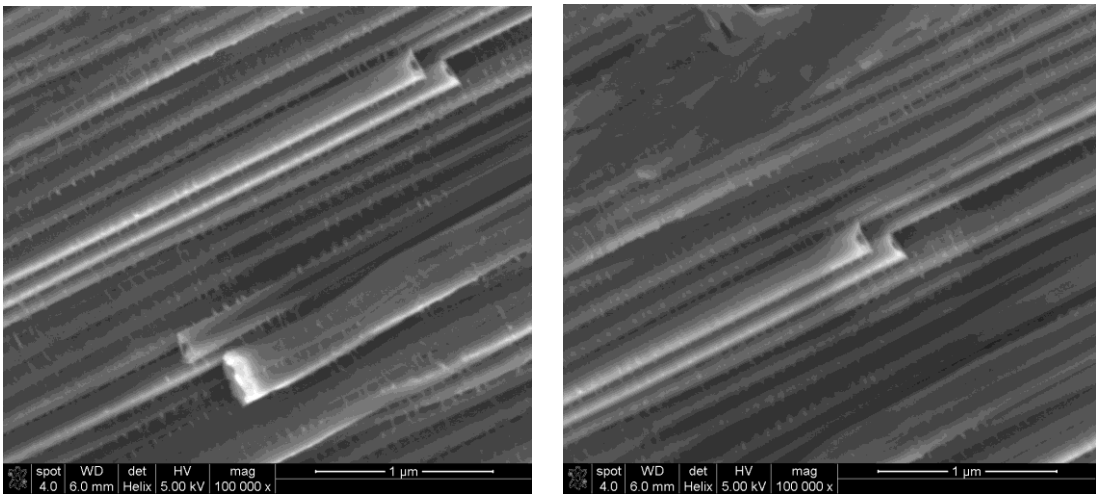

Figure 6. SEM images of TiO_2 nanotubes anodized at 60V for 3 h, revealing bamboo-like rings.

These structures are unique from commonly anodized nanotubes because of the bamboo-like ring formations, which seem to be growing very uniformly. Although they may not occur at fixed distances along the tubes, one can note that the rings are forming in distinct, homogeneous layers. These rings may contribute to the highly aligned and close-packed nature of the array. The nanotubes shown in figures 5 and 6 have a length of 19 µm, tube thickness of 64 nm, and a pore diameter of 32 nm. Since this was made immediately after mixing a batch of electrolyte solution (0.25 weight-percent NH_4F and 0.75% H_2O in ethylene glycol), it is possible that the NH_4F was not equally distributed. The opposite affect can be seen in figure 7, in which the uneven distribution of NH_4F right after mixing a batch of electrolyte solution resulted in extraordinarily high concentration of F^- and the complete dissolution of the titanium electrode. The high wall thickness compared to pore size is most likely due to a low concentration of F^- ions in the electrolyte solution which slowed down the dissolution rate, thus decreasing the inner diameter. Therefore, by increasing the concentration of F^- ions in the electrolyte from 0.25 weight-percent to 0.75 weight-percent, the inner diameter can be increased from 32 nm to 130 nm (shown in figure 8). The structures on the surface of the tube result from bR dye soaking.

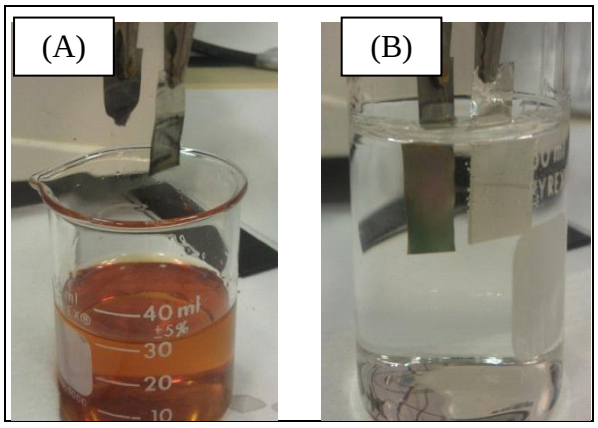

Figure 7. (A) Anodization with a high NH_4F concentration (>1%) and (B) anodization with a normal NH_4F concentration (0.25%–1%).

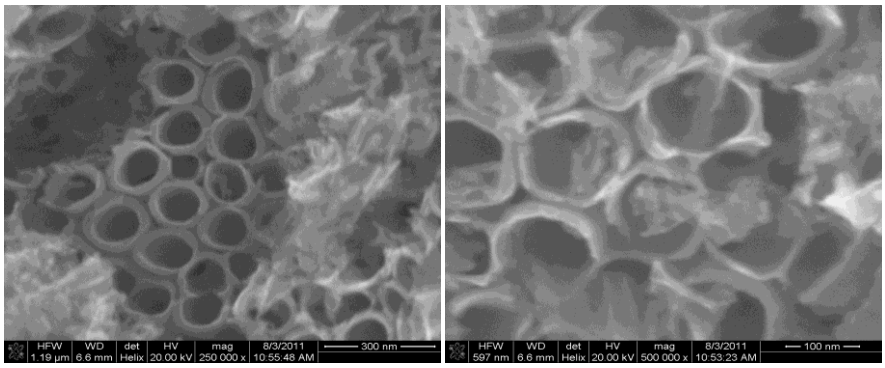

Figure 8. SEM images of nanotubes anodized at 60 V with 0.75 weight-percent NH_4F after bR soaking.

Further investigation of the effects of anodization parameters show that nanotubes arrays can be over-anodized. The SEM images in figure 9 report samples that were anodized for 6 h at 60 V, using an electrolyte consisting of 1 weight-percent NH_4F and 0.25 weight-percent H_2O. This shows the effects of electrode preparation as well as the sensitivity of the nanotubes. The SEM images report grass-like structures, also known as nano-wires, of ~24 nm thickness sitting on top of a highly porous honeycomb-like nanostructure with wall thickness of only 36 nm. The "nano-grass" is most likely the result of not mechanically polishing and sonicating the electrode prior to anodization. This, coupled with a higher concentration, allowed an accelerated chemical attack on the tube ends and the formation of nanograss. The top surface was left non-uniform due to an uneven dissolution of the titanium. The longer anodization time presumably also contributed to the rapid breakdown of the nanotubes.

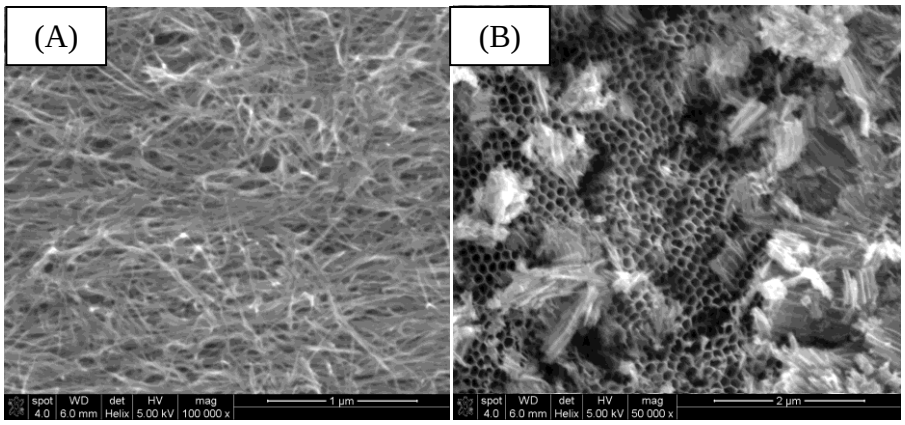

Figure 9. (A) Nanograss formations and (B) honeycomb structure anodized at 60 V for 6 h at 1% NH_4F concentration.

XRD analysis, shown in figure 10, agrees with the TiO_2 phase diagram and verifies the standard in literature that states annealing TiO_2 arrays at 450 °C at for 3 h will achieve a pure anatase structure. This is a critical step in achieving the full potential of the nanotubes.

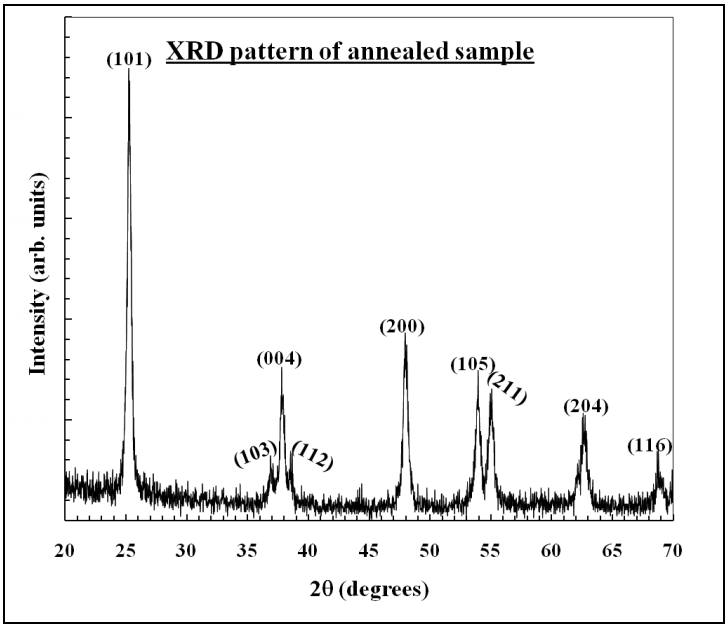

Figure 10. XRD measurement of TiO_2 nanotubes annealed at 450 °C.

Figure 11 displays voltage vs. current density readings of nanotube DSSCs. In order to evaluate the binding of bR-dye to the TiO_2 vs. the commonly used Ru-dye, a preliminary test was performed using nanotubes on their original Ti substrate. Using a Newport illuminator (model 67005) and a Keithley 6430 SourceMeter, current and voltage measurements were taken. The efficiency of the cells were determined by dividing the max power output of the cell by the input power from the illuminator. At 60 mW of illumination, the ruthenium cell and bR cell achieved efficiencies at 1.2% and 0.001%, respectively (although the current density, voltage, and overall

efficiency were fairly low). This is expected because of a thin TiO_2 layer that forms between the Ti substrate and the nanotubes array, which adversely affects the cells performance. The cell must also be illuminated through the counter-electrode because Ti is opaque, heavily reducing the amount of photons that make it to the photoanode. Furthermore, it is likely that the bR molecules were too large to effectively bind to the inner diameter of the nanotubes. There is still much promise for bacteriorhodopsin as a bio-photosensitizer because studies (*16*) have shown that it has nearly twice the absorbance of the traditionally used ruthenium dye.

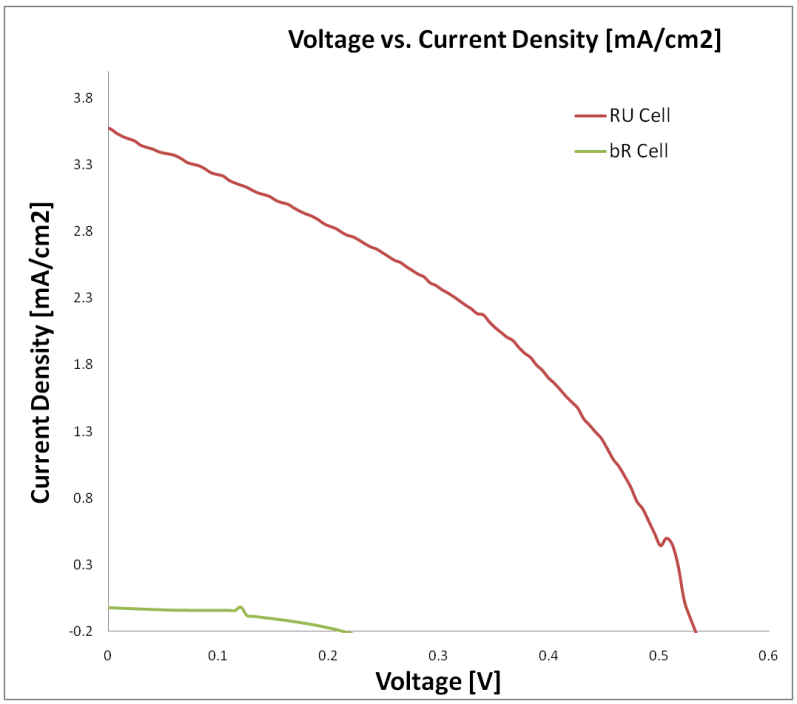

Figure 11. Voltage vs. current density of a DSSC using Ru-dye vs. a BSSC using bR.

4. Conclusion

This study presents a method of obtaining free-standing, highly organized TiO_2 arrays for use in flexible bio-sensitized solar cells. Free-standing, highly oriented and hexagonally packed nanotubes were synthesized and integrated with bacteriorhodopsin. Future efforts will be directed towards better understanding the growth mechanisms of the TiO_2 nanotube arrays, specifically with bamboo-like rings, with the goal of being able to further control nanotube growth. Combining the nanotubes with an indium tin oxide coated PET using a sol-gel consisting of Ti nanoparticles will be applied in future research and should greatly increase the performance of the solar cell. In order to improve the reported results, a higher concentration of NH_4F within the electrolyte solution should be used to increase the pore size, and

experimentation with de-lipidated bacteriorhodopsin will be conducted to allow for better integration with TiNT due to a more effective dye-sensitization. Furthermore, the binding mechanism of bR to the surface of the TiO_2 also needs to be investigated. The effects of performing a zero-length EDC linker, based off a study performed by Thavasi et al. (*16*), may possibly bind the bacteriorhodopsin to the surface of the TiO_2 nanotubes more effectively than traditional dye soaking. This could potentially increase the surface density, thereby increasing the potential of bacteriorhodopsin as a sensitizer. Finally, it is also important to note that although the nanograss and honeycomb structures grown in this study may not be ideal for use in a DSSC, they could be potentially useful for applications such as bacteria filters, bio-sensors, and various other biomedical applications.

5. References

1. Kang, M. G.; Park, N.-G.; Ryu, K. S.; Chang, S. H. A 4.2% Efficient Flexible Dye-Sensitized TiO_2 Solar Cells using Stainless Steel Substrate. *Solar Energy Materials and Solar Cells* **2006**, 90, 574–581.

2. Grätzel, M. Solar Energy Conversion by Dye-Sensitized Solar Cells. *Inorg. Chem.* **2005**, *44*, 6841–6841.

3. Jennings, J. R.; Ghicov, A.; Peter, L.; Schumuki, P.; Walker, A. Dye-Sensitized Solar Cells Based on Oriented TiO_2 Nanotube Arrays: Transport, Trapping, and Transfer of Electrons. *J. Am. Chem. Soc.* **2008**, *130*, 13364–13372.

4. Chiba, Y.; Islam, A.; Watanabe, Y.; Komiya, R.; Koide, N.; Han, L. Dye-Sensitized Solar Cells with Conversion Efficiency of 11.1%. *Jpn. J. Appl. Phys*. **2006**, *45*, L638-L640.

5. Koops, S. E.; O'Regan, B. C.; Barnes, P. R. F.; Durrant, J. R. Parameters Influencing the Efficiency of Electron Injection in Dye-Sensitized Solar Cells. *J. Am. Chem. Soc*. **2009**, *131*, 4808–4818.

6. Nelson, J. Continuous Time Random Walk Model of Electron Transport in Nanocrystalline TiO_2 Electrodes. *Phys. Rev. B: Condens. Matter Mater. Phys*. **1999**, *59*, 15374.

7. Shankar, K.; Mor, G. K.; Prakasam, H. E.; Varghese, O. K.; Grimes, C. A. Self-Assembled Hybrid Polymer TiO_2 Nanotube Array Heterojunction Solar Cells. *Lamguir* **2007**, *23*, 12444–12449.

8. Zhu, K.; Neale, N. R.; Miedaner, A.; Frank, A. J. Enhanced Charge-Collection Efficiencies and Light Scattering in Dye-Sensitized Solar Cells Using Oriented TiO_2 Nanotube Arrays. *Nano. Lett.* **2007**, *7*, 69–74.

9. Elsanousi, A.; Zhang; J. Self-Organized $Ti0_2$ Nanotubes with Controlled Dimensions by Anodic Oxidation. *J. Mater. Sci*. **2008**, *43*, 7219–7729.

10. Ghicov, A.; Albu, S. TiO_2 Nanotubes in Dye-Sensitized Solar Cells: Critical Factors for the Conversion Efficiency. *Chem. Asian J.* **2009**, *4*, 520–525.

11. Cai, Q.; Paulose, M.; Varghese, O. K. The Effect of Electrolyte Composition on the Fabrication of Self-Organized Titanium Oxide Nanotube Arrays by Anodic Oxidation. *J. Mater. Res.* **2005**, 20, 230–236.

12. Macak, J. M.; Schumuki, P. Anodic Growth of Self-Organized Anodic TiO_2 Nanotubes in Vixcous Electrolytes. *J. Electroceram*. **2006**, 52, 1258–1264.

13. Mor G. K.; Carvalho, M. A.; Varghese, O. K.; Pishko, M. V.; Grimes, C. A. A Room Temperature TiO_2 Nanotube Hydrogen Sensor Able to Self-Clean Photoactively from Environmental Contamination. *J. Mater. Sci.* **2004**, *19*, 628–634.

14. Prakasam, H. E.; Shankar, K.; Paulose, M.; Varghese, O. K.; Grimes, C. A. A New Benchmark for TiO_2 Nanotube Array Growth by Anodization. *J. Phys. Chem.* **2007**, *111*, 7235–7241.

15. Park, N. G.; Frank, A. J. Comparison of Dye-Sensitized Rutile and Anatase-Based TiO_2 Solar Cells. *J. Phys. Chem. B* **2000**, *104, 8989–8994*.

16. Thavasi V.; Lazarova T.; Filipek, S.; Kolinski, M.; Querol, E.; Kumar, A.; Ramakrishna, S.; Padros, E.; Renugopalakrishnan, V. Study on the Feasibility of Bacteriorhodopsin as Bio-Photosensitizer in Excitonic Solar Cell: A First Report. *J. Nano*. **2009**, *9*, 1679–1687.

17. Lei, B.; Liao, J.; Wang, R. J.; Su, C.; Kuang, D. Ordered Crystalline $Ti0_2$ Nanotube Arrays on Transparent FTO Glass for Efficient Dye-Sensitized Solar Cells. *J. Phys. Chem.* C **2010**, *114*, 15528–33.

18. Yang D. J.; Kim, H. G.; Cho, S. J.; Choi, W. Y. Thickness-Conversion Ratio from Titanium to TiO_2 Nanotube Fabricated by Anodization Method. *Mater. Lett*. **2008**, 62, 775–779.

19. Macak J. M.; Tsuchiya, H.; Ghicov, A.; Yashuda, K.; Schumuki, P. TiO_2 Nanotubes: Self-Organized Electrochemical Formation, Properties, and Applications. *Curr. Opin. Solid State Mater. Sci*. **2007**, 11, 3–18.

NO. OF COPIES	ORGANIZATION
1 (PDF only)	DEFENSE TECHNICAL INFORMATION CTR DTIC OCA 8725 JOHN J KINGMAN RD STE 0944 FORT BELVOIR VA 22060-6218
1	DIRECTOR US ARMY RESEARCH LAB IMNE ALC HRR 2800 POWDER MILL RD ADELPHI MD 20783-1197
1	DIRECTOR US ARMY RESEARCH LAB RDRL CIO LL 2800 POWDER MILL RD ADELPHI MD 20783-1197

NO. OF
COPIES ORGANIZATION

ABERDEEN PROVING GROUND

16 DIR USARL
RDRL WM
S KARNA (5 CPS)
J MCCAULEY
RDRL WMM A
MARK GRIEP (10 CPS)